

AN INTERFACE TO QUANTUM ESPRESSO

Linu Malakkal¹, Barbara Szpunar², Juan Carlos Zuniga³, Ravi Kiran Siripurapu¹, Jerzy A. Szpunar¹

¹Department of Mechanical Engineering, University of Saskatchewan

²Department of Physics and Engineering Physics, University of Saskatchewan

³Information and communications technology, research computing, University of Saskatchewan

Keywords: Quantum ESPRESSO, QE-nipy-advanced, First principle calculation, Slack thermal conductivity, Nuclear Materials, Silicon carbide, Thoria, Zirconia

Abstract

Our project aims at providing the materials engineering fraternity with a simple and effective interface using ipython to operate Quantum ESPRESSO (QE), an open source code for materials simulation. QE is a first principles code using density functional theory, plane waves and pseudo potentials; it has ability to predict material properties. Ipython notebook interface uses the scope of the following libraries; Atomic Simulation Environment (ASE), matplotlib, scipy, numpy, pysglib, elastic and newly developed library: QE-nipy-advanced to predict the properties. QE-nipy-advanced is the latest version of QE-nipy. The latest version incorporates features that can take care of all the input parameters supported by PWscf and PHonon packages of Quantum ESPRESSO. Thermo-mechanical properties of some nuclear materials with different magnetic and metallic behavior has been studied using the QE-nipy-advanced, but in here we demonstrate the thermo-mechanical properties of non-magnetic insulator like silicon carbide and thoria, which are materials for future nuclear reactor applications.

Introduction

QE-nipy-advanced, python and ipython software has been developed to facilitate the ongoing nuclear research, as this user-friendly interface can be used by graduate and undergraduate students of to study the properties of materials. The interface has been developed based on the ipython interactive notebook that allow direct access to the Quantum ESPRESSO code [1], without the need to use a Unix/Linux environment and rather complex details of job queuing and submission procedure. The users can utilize the scope of libraries such as ASE, matplotlib, scipy, numpy and QE-nipy-advanced scripts to build the input files and view the outputs of simulations, and perform calculation on the remote clusters where Quantum ESPRESSO code is installed. The exemplary tasks performed by the interface includes geometry optimization, electronic structure calculations, calculation of phonon density of states and elastic constants calculation. The properties derived from these calculations include lattice constant, elastic constants, bulk modulus, poisson ratio, heat capacity (C_v), entropy (S) and thermal expansion as a function of temperature. Further, a FORTRAN code build on Slack model [2] is used in predicting the thermal conductivity using properties that are listed above.

After Fukushima accident the major focus of nuclear researchers have been on the development of enhanced accident tolerant fuel. The major characteristic of such fuels is high conductivity that will allow the reactor core to withstand the loss of coolant for longer time period. Higher thermal conductivity of fuel/cladding system will also decrease temperature in the centerline and temperature gradient in the fuel resulting in reduced fission gas release. Reduction of thermal stress

will allow to improve the resistance of pellet to cracking [3]. Various materials with better thermal conductivity than the current fuel/cladding materials are under consideration for the next generation nuclear reactors. Silicon carbide (SiC) is considered because of its high thermal conductivity, high melting point, good chemical stability, low neutron cross-section and low swelling rate [4]. It is therefore an excellent candidate for both composite fuel (UO₂-SiC) and ceramic cladding. With India unveiling their latest design for a novel 300 MW thorium fueled Advanced Heavy Water Reactor (AWHR) there has been an interest in thoria as well. For this reason a systematic study of thermo-mechanical properties of silicon carbide and thoria is carried out using Quantum ESPRESSO.

In this paper we will briefly describe how the interface works and the thermo-mechanical properties of silicon carbide and thoria are calculated. In section 2, we describe the graphical outline of interface work and the methodology used for property prediction. In section 3, we will present more computational details. Finally, we describe the results of calculation of silicon carbide in details and compare the thermal conductivity of thoria and silicon carbide.

Methodology

In this Section, we briefly describe how the scope of various libraries are used, the modules in QE-nipy-advanced and methodology used to calculate thermo-mechanical properties.

2.1) How the interface works.

The libraries include Atomic Simulation Environment (ASE), NumPy, SciPy, matplotlib and pypglib. The modules crystal.py and atom.py of ASE are imported to generate the crystalline structure and to setup atoms in electronic structure respectively. The Pypglib is the module used to find and handle crystal symmetries. The arrays and the mathematical function of these arrays are taken care by the module NumPy and SciPy, an extension to python programming language.

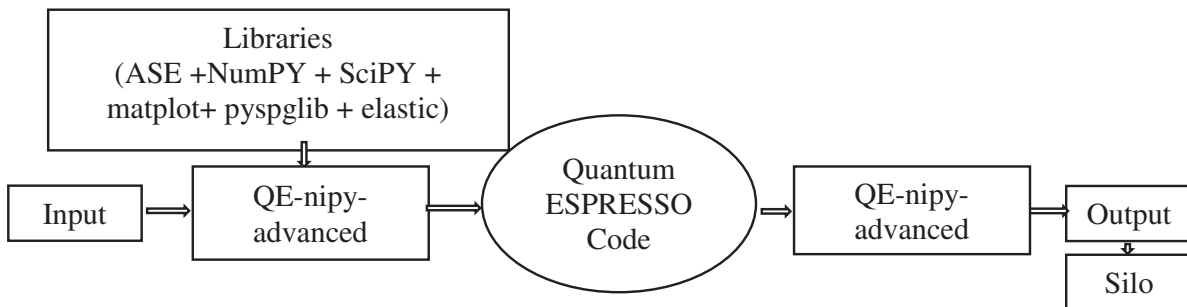


Figure1. Pictorial description of how various libraries and QE-nipy-advanced are connected.

The initial version of software with rather limited applications: QE-nipy was developed by Pawel Jochym during his visit at the University of Saskatchewan. It was based on the early works by Nikolay Markovskiy, Alexander Dementsoy and Luca Tornatore. The elastic module, developed in python, is an adaptation of the VASP version [5] to QE. Though the modules and the functionality of the modules like writers.py, analyzer.py, qeio.py, readers.py and quantumespresso.py are similar as in QE-nipy, various modifications in these modules has been done to add the extra features in QE-nipy-advanced and overcome the restrictions in application. The writers.py creates the input file needed for Quantum Espresso. The output generated is read by the qeio.py and then analysed with analyser.py. The results in graphical form are generated in

the ipython notebook using the library matplotlib. The computed properties are stored in Silo large scale disc storage facility at the University of Saskatchewan.

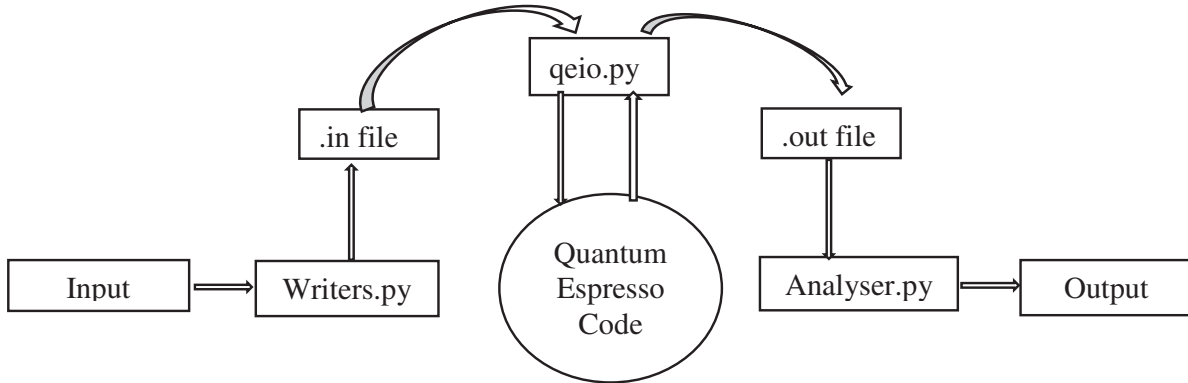


Figure 2. Functionalities of modules in QE-nipy-advanced

2.2 Evaluation of 0 K temperature properties

Geometry optimization is carried out to evaluate the structural properties at zero Kelvin temperature by minimizing the total energy by varying cell parameter and atomic positions. The ground state structural properties are also evaluated by fitting Birch-Murnaghan equation of state [6] and that is implemented in QE-nipy-advanced by importing the elastic module. The elastic constants can be calculated using the stress-strain method [7]. From the elastic constants the bulk (B) and shear (G) modulus can be derived. The Hill average and Voigt [8] and Reuss [9] methods are used in calculation. We analyze here cubic, polycrystalline structure therefore Young's modulus (Y) can be evaluated assuming an isotropic aggregate of grains with non-isotropic elastic properties, as a result we will have:

$$Y = \frac{9BG}{3B + G} \quad (1)$$

The Poisson's ratio is calculated as:

$$\eta = \frac{3B - 2G}{2(3B + G)} \quad (2)$$

2.3 Lattice dynamics in Quasi-harmonic approximation

Phonon density of states is obtained using density functional perturbation theory (DFPT) as implemented in Quantum ESPRESSO [1]. Phonon contribution to thermodynamic properties is calculated within quasi-harmonic approximation. The analyser.py of QE-nipy-advanced uses the phonon density of states to obtain the thermodynamic properties. The equations used by analyzer.py are described below.

2.3.1 Thermal Expansion: The Helmholtz free energy at volume V was calculated as a sum of the electronic energy (E (V)) and vibrational energy $F_{\text{vib}} (V, T)$ for a given volume V and temperature T:

$$F(V, T) = E(V) + F_{\text{vib}}(V, T) \quad (3)$$

We assume that for insulators the electronic entropy can be neglected. The vibrational Helmholtz free energy is calculated as described before [10,11] by evaluating phonons density of states at

different volume and integrating the energy of phonons ($\hbar\omega$) over the density of states ($\rho(\omega)$) and weighting it by the temperature dependent Boltzmann factor.

$$F_{\text{ph}}(V, T) = k_B T \int_{\omega_{\text{min}}}^{\omega_{\text{max}}} \rho(\omega) \ln \left[2 \sinh \left(\frac{\hbar\omega}{2k_B T} \right) \right] d\omega \quad (4)$$

where k_B is the Boltzmann constant. The equilibrium volume at each temperature was calculated by fitting the free energy to the Birch-Murnaghan equation of state.

$$F(V, T) = F_0(T) + \frac{B_0(T)V}{B_0'(T)} \left[\frac{\left(\frac{V_0(T)}{V} \right)^{B_0'(T)}}{B_0'(T) - 1} \right] - \frac{B_0(T)V}{B_0'(T) - 1} \quad (5)$$

Where $F_0(T)$, $B_0(T)$ are the values of the total free energy and bulk modulus, for the equilibrium primitive unit cell volume: $V_0(T)$ at the temperature T . The equilibrium lattice constant for the conventional unit cell is calculated at each temperature from the conventional unit cell volume (for FCC structure four times larger than primitive volume) as:

$$a^c(T) = (V_0^c)^{1/3} \quad (6)$$

The linear and volume thermal expansion coefficients are related and therefore can be calculated from each other at constant pressure (P):

$$\alpha(T)_P = \frac{1}{L} \left(\frac{\partial L}{\partial T} \right)_P = \frac{1}{3V_0} \left(\frac{\partial V_0}{\partial T} \right)_P \quad (7)$$

2.3.2 Heat Capacity: The heat capacity is calculated using the equation (8), where N_A is Avogadro number, k_B is the Boltzmann constant and $\rho(\omega)$ is the density of states of phonons (with $\hbar\omega$ energy) per primitive unit cell. Note that heat capacity at constant volume remains constant at higher temperatures.

$$C_v(T) = N_A k_B \int_{\omega_{\text{min}}}^{\omega_{\text{max}}} \frac{\left(\frac{\hbar\omega}{k_B T} \right)^2 \exp \left(\frac{\hbar\omega}{k_B T} \right)}{\left[\exp \left(\frac{\hbar\omega}{k_B T} \right) - 1 \right]^2} \rho(\omega) d\omega \quad (8)$$

2.4 Thermal conductivity: Lattice thermal conductivity of SiC and ThO₂ is evaluated using the Slack model [2], which is given by the equation

$$\kappa_L = \frac{C\theta(T)^3 M_M V(T)^{1/3}}{(n\gamma(T))^2 T} \quad (9)$$

where C is equal to $3.04 \times 10^4 \text{ Wm}^{-2}\text{K}^{-1} \text{ g}^{-1} \text{ mol}$ and M_M molar mass per primitive cell (40.096 and 264 g mol^{-1} for SiC and ThO₂ respectively) and $V(T)$ the volume of the primitive cell, but in cubic m. $\gamma(T)$ is the Grüneisen parameter and $\theta(T)$ is Debye temperature. The Grüneisen parameter is calculated using equation (10).

$$\gamma(T) = \frac{3\alpha(T)V_M(T)}{C_v(T)\beta(T)} \quad (10)$$

Where $\alpha(T)$, $V_M(T)$, $C_V(T)$, $\beta(T)$ are linear thermal expansion, molar volume, the heat capacity at constant volume per mol and compressibility respectively are calculated as described above. Debye temperature (θ in K) within the isotropic approximation [12] (in atomic units: $m = \hbar = e = 1$) is given by equation (11), where M is the mass, n is the number of atoms per primitive cell (2 for SiC and 3 for ThO₂) with its volume $V(T)$ (calculated using $a(T)$ derived above) and $f(\eta(T))$ is the scaling function calculated using equation (12).

$$\theta(T) = \frac{(6\pi^2 V(T)^{1/2} n)^{1/3} f(\eta(T))}{k_B (\beta(T) M)^{1/2}} \quad (11)$$

The Poisson's ratio (η) as a function of temperature is evaluated by Eq. 2 using the calculated shear and Young moduli.

$$f(\eta) = 3^{1/3} \left[2 \left(\frac{2}{3} \frac{1+\eta}{1-2\eta} \right)^{3/2} + \left(\frac{1}{3} \frac{1+\eta}{1-\eta} \right)^{3/2} \right]^{-1/3} \quad (12)$$

Computational Details

The calculation of cubic SiC was carried out implementing density functional theory within a Perdew-Zunger (Local Density Approximation). The structural and mechanical properties have been calculated using a kinetic energy cutoff of 70 Ry over a Brillouin zone integration of 8x8x8 mesh. The dynamical matrices were calculated on a mesh of 4x4x4 q-points in the irreducible Brillouin zone. In case of ThO₂ recently proposed GGA functional for solids, PBEsol was used with the pseudo-potentials generated using opium code for PBE functional. The kinetic energy cut-off of 70 Ryd and Brillouin zone integration was performed on a Monkhorst-Pack 8x8x8. For the Lattice dynamic calculation the dynamical matrices were calculated on a 4x4x4 mesh.

Results and Discussion

4.1 Ground state properties

The ground state properties of both SiC and Thoria in cubic structure are listed in Table 1. The results were compared with experiment and shows good agreement.

Table 1. Ground state structural properties of SiC and ThO₂

Properties	SiC		ThO ₂	
	This work.	Expt.	This work	Expt.
Lattice Constant	4.3342	4.3596 [13]	5.53	5.598 [15]
Bulk Modulus	224.4	224 [14]	202.8	223 [16], 193 [17,18]
Elastic constant {C ₁₁ ,C ₁₂ ,C ₄₄ }	400, 140, 279	390, 142, 256 [14]	379,117, 87	377, 146,89 [16]

4.2. Phonon Dispersion

The phonon dispersion measurement, a key step in measuring phonon-assisted properties are described in figure 3, for 3C-SiC along high symmetry lines in the Brillouin zone of the FCC structure. The measured value was in good agreement with the experimental data by J.Serrano et.al [19] that were obtained for the entire Brillouin zone by inelastic x-ray scattering using a synchrotron radiation source. The image shown in figure 3 is generated by the interface using

matplotlib library. The calculated phonon dispersion curves for thoria was also in good agreement with experiment.

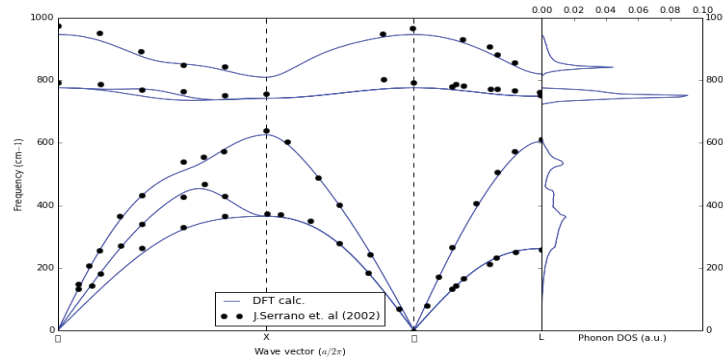


Figure 3. Calculated phonon dispersion curves and density of states for cubic SiC.

4.3 Thermal Properties

Volume thermal expansion, heat capacity, lattice constant and entropy as a function of temperature is calculated and shows good comparison with experiment as shown in figure 4 and 5 for SiC. Similar calculation for thoria also showed good agreement with experiment.

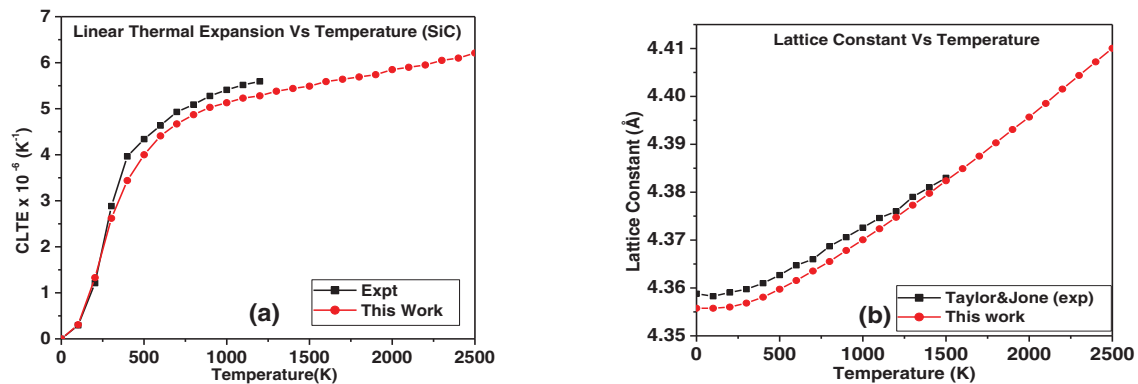


Figure 4. The calculated thermal expansion of SiC versus experimental data: a) Coefficient of Linear thermal expansion and b) Lattice constant as a function of temperature. The experimental results shown in figure (a) and (b) are from reference [21] [22] respectively.

4.4 Thermal conductivity (κ_L)

In spite of many research papers on SiC the thermal conductivity (κ_L) of cubic SiC using first principle calculation was not reported. In this work we have calculated κ_L up to 1000 K using the Slack model and the data are compared with the experiment carried out by Senor et al [23] and Taylor et.al [24] as shown in figure 6 (a). Even though the theoretical prediction of κ_L are higher than the experiment, the trend remains the same. The theoretical curve probably represent the upper limit of κ_L . The difference between the experiment and theoretical calculation is partly caused by the impurities in the SiC and also the limitations of theoretical prediction of the thermal expansion accurately. It is worthwhile to note that the theoretical κ_L result for 6H SiC are very close to the experimental [25] and is shown in inset of figure 6(a).It was noted previously [10, 26] and we also confirmed it in our paper [27] that the phonon contribution to the κ_L of thoria can be well reproduced using a simplified Slack model. Therefore we have explored its application even

further using the thermal expansion ($\alpha(T)$, $a(T)$) and the adiabatic elastic moduli evaluated as described above.

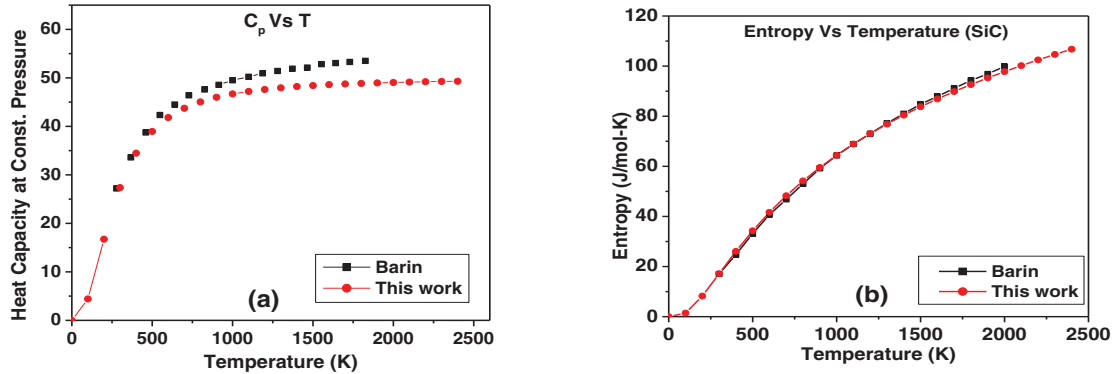


Figure 5. SiC: (a) heat capacity and (b) entropy as a function of temperature. Experimental results are from the reference [21], [22] for figure (a) and (b) respectively.

We also compared the κ_L of thoria with experiment (figure (6b)) [28] and agreement with experiment is very good. We also performed calculations for the cubic ZrO_2 that exist only at high temperature and as shown in figure (18) and (19) of Ref. [2] at 2000 K has κ_L about $2 \text{ Wm}^{-1}\text{K}^{-1}$ and very close to the κ_L of thoria at the same temperature. However zirconia structure at presented in figure 6 (b) temperature range is monoclinic and it is known as having low κ_L . It is therefore interesting that pure cubic zirconia would have much higher κ_L which is only slightly lower than thoria.

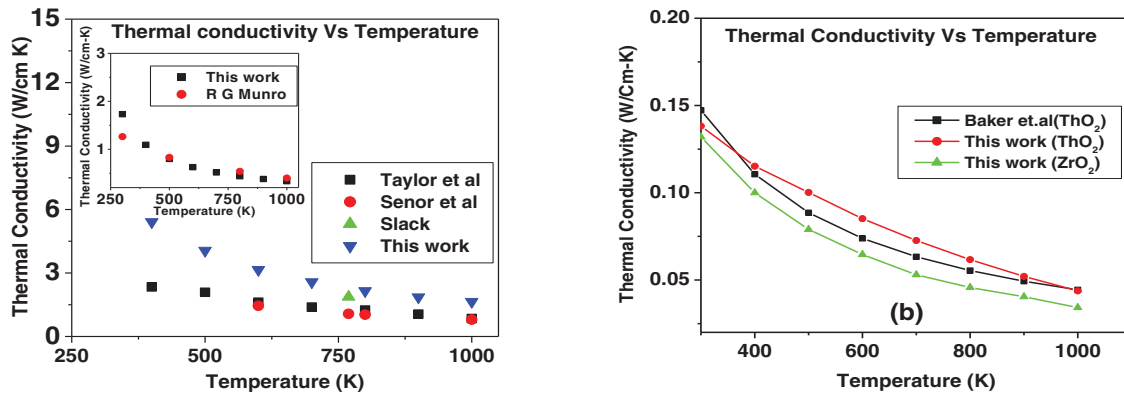


Figure 6. (a) Thermal Conductivity SiC and (b) ThO₂ compared with pure cubic ZrO₂

Summary

In summary, we were successfully able to calculate the thermo-mechanical properties of SiC and ThO₂ using Quantum ESPRESSO code by implementing the QE-nipy-advanced Interface. The thermal conductivities of SiC and ThO₂ calculated using Slack model up to 1000 K are also in agreement with experiment. The thermal conductivity is related to structure and hypothetical pure cubic zirconia would have good thermal conductivity. Presented example demonstrates application of Quantum ESPRESSO for prediction of thermo-physical properties of new materials.

Acknowledgement

We acknowledge access to high performance supercomputers Compute Canada and Plato at the University of Saskatchewan and the initial developmental work by P. Jochym during his visit at

the University of Saskatchewan. The previous similar developments of QECalc by Nikolay Markovskiy, Alexander Dementsov and development of ase qe interface by Luca Tornatore is acknowledged. This work was supported by grant from the National Sciences and Engineering Research Council of Canada

References

- [1]. P. Giannozzi, S. Baroni et.al. "QUANTUM ESPRESSO: a modular and open-source software project for quantum simulations of Materials," *Journal of Physics: Condensed Matter*, 21 (2009), 395502- 395521
- [2] G.A. Slack, "The Thermal conductivity of Nonmetallic crystals," *Solid State Physics*, 34 (1979), 1-71
- [3] A.Griffith, "Accident Tolerant Fuels" (Report USNRC, DOE, 2013)
- [4] J.A. Khan, T.W. Knight, S.B Pakala, W. Jiang, R. Fang, and J. S. Tulenko, "Enhanced thermal Conductivity for LWR Fuel," *Journal Nuclear Technology*, 169 (2010), 61-72
- [5] P.T. Jochym and K. Parlinski, Ab initio lattice dynamics and elastic constants of ZrC, *European Physical Journal B*, 15, 2 (2000) 265-268
- [6] F. D. Murnaghan, "The Compressibility of Media under Extreme Pressures," *Proceedings of the National Academy of Sciences of the United States of America*, 30 (1944), 244-247
- [7]. L.D. Landau, E.M. Lifszyc, *Theory of elasticity*, (Pergamon Press, 1970)
- [8] W. Voigt, "*Lehrbuch der Kristallphysik*," 1928, 962
- [9] A. Reuss, "*Berechnung der Fließgrenze von Mischkristallen auf Grund der Plastizitätsbedingung für Einkristalle*," *Z Angew Math Mech*, 9 (1929), 49-58
- [10] H. Y. Xiao, Y. Zhang, and W. J. Weber, "Thermodynamic Properties of $Ce_xTh_{1-x}O_2$ Solid Solution from First-Principles Calculations," *Acta Materialia*, 61 (2013), 467-476.
- [11]. Y. Lu, Y. Yang and P. Zhang, "Thermodynamic properties and structural stability of thorium dioxide," *Journal of Physics: Condensed Matter*, 24 (2012), 225801-225811.
- [12] M.A. Blanco, E. Francisco, V. Luaña, "GIBBS: isothermal-isobaric thermodynamics of solids from energy curves using a quasi-harmonic Debye model" *Computer Physics Communications*, 158 (2004), 57-72
- [13]. P. E. Van Camp, V. E. Van Doren, and J. T. Devreese, "First-principles calculation of the pressure coefficient of the indirect band gap and of the charge density of C and Si," *Physical Review B*, 34 (1986), 1314-1316
- [14] W. R. L. Lambrecht, B. Segall, M. Methfessel, and M. van Schilfgaarde, "Calculated elastic constants and deformation potentials of cubic SiC," *Physical Review B*, 44 (1991), 3685-3694
- [15] J. Staun Olsen, L. Gerward, V. Kanchana and G. Vaitheeswaran, "Erratum to "The bulk modulus of ThO₂—an experimental and theoretical study", *Journal of Alloys and Compounds*, 381 (2004) 37-40
- [16] K.K. Phani, D.sanyal, "Elastic properties of porous polycrystalline thoria—A relook," *Journal of European Ceramic Society*, 29(3) (2009), 385-390
- [17] P.M. Macedo, W. Capps, J.B. Watchman, "Elastic Constants of Single Crystal ThO₂ at 25°C," *Journal of the American Ceramic Society*, 47 (1964), 651-1.
- [18] J. Serrano, J.Stremper, M. Cardona, M. Schwoerer-Böhning, H. Requardt, M. Lorenzen. B. Stojetz, P. Pavaone and W.J.Choyke, "Determination of the phonon dispersion of zinc blende (3C) silicon carbide by inelastic x-ray scattering," *Applied Physics Letters*, 80 (2002), 4360-4362.
- [19] A. Sparavigna, "Lattice thermal conductivity in cubic silicon carbide," *Physical Review B*, 66 (2002),174301 (5).
- [20] K. Karch, P. Pavone, W. Windl, O. Schütt, and D. Strauch, "Ab initio calculation of structural and lattice-dynamical properties of silicon carbide," *Physical Review B*, 50(1994), 17054 (10)
- [21] Taylor, A., Jones, R.M. in *Silicon Carbide - A High Temperature Semiconductor*, Eds. O'Connor, J.R., Smiltens, J., Pergamon Press, Oxford, London, New York, Paris 1960, 147
- [22] I.Barin, *Thermochemical Data of Pure Substances* (Newyork, 1995),
- [23] R.E. Taylor, H. Groot, J. Ferrier, "*Thermophysical Properties Research Laboratory*" (Report TRPL 1336, 1993)
- [24] D. J. Senior, G. E. Youngblood, C. E. Moore, D. J. Trimble, G. A. Newsome and J. J. Woods, "Effects of neutron irradiation on thermal conductivity of SiC-based composites and monolithic ceramics," *Fusion Technology* "30(3), (1996), 943-955.
- [25] R.G.Munro "Materials Properties of a Sintered ∞ -SiC," *American Institute of Physics and American Chemical Society* (1997), 1195-1201.
- [26] J.K Fink, "Thermophysical properties of uranium dioxide," *Journal of Nuclear Materials*, 279 (2000), 1-18
- [27] B.Szpunar, J A Szpunar, "Theoretical investigation of structural and thermo-mechanical properties of thoria up to 3300 K temperature," *Solid State Sciences*, 28 (2014), 36-40
- [28] K. Bakker, E. H. P. Cordfunke, R. J. M. Konings, and R. P. C. Schram, "Critical Evaluation of the thermal properties of ThO₂ and Th_{1-y}U_yO₂ and a survey of the literature Data on Th_{1-y}Pu_yO₂," *Journal of Nuclear Materials*, 250 (1997), 1-12